DISTRIBUTED ZERO-DELAY JOINT SOURCE-CHANNEL CODING FOR A BI-VARIATE GAUSSIAN ON A GAUSSIAN MAC

Pål Anders Floor [∗#1], *Anna N. Kim* [#2] *Niklas Wernersson* [†],
Tor A. Ramstad [#], *Mikael Skoglund* [‡], *Ilangko Balasingham* [∗#]

[∗]Intervention Center, Oslo University Hospital and Institute of Clinical Medicine, University of Oslo, Oslo, Norway.
[1]andflo@rr.research.no
[#] Dept. of Electronics and Telecommunications, Norwegian University of Science and Technology, Trondheim, Norway.
[2]annak@iet.ntnu.no
[†] Ericsson Research, Stockholm, Sweden.
[‡] School of Electrical Engineering and the ACCESS Linnaeus Center, Royal Institute of Technology, Stockholm, Sweden.

ABSTRACT

In this paper delay-free distributed joint source-channel coding for communication of two correlated Gaussian sources over a Gaussian Multiple Access Channel (GMAC) are considered. Both discrete and hybrid discrete analog schemes are proposed and optimized. The proposed schemes are noise robust and show promising performance which improve with increasing correlation.

1. BACKGROUND AND FORMULATION

In the recent work of [1], the distortion lower bound was determined for transmitting a bi-variate Gaussian source over a Gaussian multiple access channel (GMAC), where each source is to be recovered at the receiver. The authors showed that below a certain channel signal-to-noise ratio (SNR) threshold, distributed uncoded transmission, where the source symbols are simply scaled to meet the channel power constraint and then transmitted directly over the channel, is able to reach the distortion lower bound. In order to get closer to the distortion lower bound for all SNR the authors further proposed a distributed scheme where each encoder consists of an infinite dimensional vector quantizer (VQ) preserving correlation superimposed on a linear mapping. It was shown that this joint source-channel coding (JSCC) approach performs very close to the the distortion lower bound for all SNR. Separate source channel coding (SSCC) on the other hand was shown to be strictly sub-optimal both to the lower bound and the proposed JSCC scheme even with infinite block length.

In a practical setting, however, infinite dimension coders are unrealistic and high dimensional coding also result in high complexity and delay which may not be desirable in certain applications. In this paper, we study the same communication problem as presented in [1], however with an added constraint - zero delay. In other words, we restrict the dimensionality of the encoding process to operate on a symbol-to-symbol basis. To our knowledge, there is no prior work that addresses such a constraint within the context of recovering *both sources* transmitted over a GMAC. We emphasize that this problem should not be confused with that of recovering the common information of the two sources, where uncoded transmission is in fact optimal for all channel SNR [2]. Naturally, one must expect that the optimal performance in our case backs off from the distortion lower bound proposed in [1], possibly at a significant amount. Nonetheless, we are interested in devising very simple, possibly implementable coding schemes under this constraint and show how they perform with respect to the distortion lower bound.

For the remaining part of this section, we present a proper definition of the communication problem. In Section 2, we describe in detail two distributed zero-delay JSCC schemes, where the first is based on *Nested Quantization* (NQ) [3], and the second is a hybrid scheme consisting of a scalar quantizer and a linear coder: *Scalar Quantizer Linear Coder* (SQLC). Both schemes are optimized based on derived distortion- and power expressions. Their simulated performance is shown in Section 3, followed by a summary.

1.1 Problem Formulation

The communication system is illustrated in Figure 1.

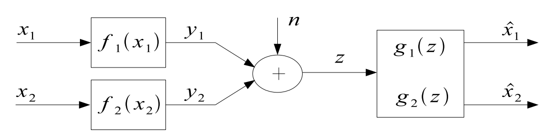

Figure 1: A Bi-variate Gaussian transmitted on a GMAC where each observation is reconstructed at the receiver.

The sources x_1 and x_2 are zero mean Gaussian random variables with variance σ_x^2 and an inter-correlation $\rho_x = \mathbf{E}[x_1 x_2]/\sigma_x^2$. The joint probability density function (pdf) is

$$p_{\mathbf{x}}(\mathbf{x}) = p_{\mathbf{x}}(x_1,x_2) = \frac{1}{2\pi\sqrt{\det(C_x)}} e^{-\frac{1}{2}\mathbf{x}^T C_x^{-1}\mathbf{x}} \qquad (1)$$

with equal marginal distributions $p_x(x_i) \sim \mathscr{N}(0,\sigma_x^2)$, and C_x is the covariance matrix. Denote the encoding functions by $f_i(x_i)$ and channel input symbols y_i, where $y_i = f_i(x_i), i = 1,2$. We define the average transmit power as $P_i = \mathbf{E}[|y_i|^2], i = 1,2$. The encoded observations are communicated over a memoryless GMAC with Gaussian additive noise of zero mean and variance σ_n^2. We assume ideal Nyquist sampling and an ideal Nyquist channel where the sampling rate of each source is the same as the signalling rate of the channel. We also assume ideal synchronization and timing between all nodes. The received signal, $z = f_1(x_1) + f_2(x_2) + n$, is passed through the decoding functions $g_i(z), i = 1,2$ to reconstruct each individual source. We use the mean-squared-error distortion criterion, and define the *average* end-to-end distortion as:

$$D = \frac{1}{2}(D_1 + D_2) = \frac{1}{2}\left(\mathbf{E}\{|x_1 - \hat{x}_1|^2\} + \mathbf{E}\{|x_2 - \hat{x}_2|^2\}\right). \quad (2)$$

The objective is to determine the memoryless mapping functions f_i and g_i, for a given power constraint, such that D is minimized. We will in this paper measure performance in terms of signal-to-distortion ratio SDR$= \sigma_x^2/D$.

We consider mainly a received power constraint [4] P_{Rx} in this paper. It is defined as $\mathbf{E}[|z|^2] \leq P_{Rx} + \sigma_n^2$. Such a constraint is meaningful when there is a strict power requirement at the receiver. As shown in [1], the received power relates to the average transmit power P_i through $P_{Rx} = P_1 + P_2 + 2\rho_x\sqrt{P_1 P_2}$. It will also become clear from Section 2 that optimization for the transmit power P_i is not advantageous due to the inherent structures of our proposed scheme. However equal transmit power, i.e. when $P_1 = P_2 = P$, is still possible using the same coder designed for P_{Rx} through time sharing.

2. DISTRIBUTED ZERO DELAY JSCC

One primary concern in our design, is that we have to ensure that the interfering sources can be split apart at the receiver. One classic approach is sequential decoding. For it to work in a zero-delay JSCC setting, we borrow the idea from *Nested Quantization* (NQ) [3].

2.1 Nested Quantization

NQ consists of two quantizers, one for each encoder. For decoding to be possible, one of the quantizers must be placed/nested in between the centroids of the other in such a way that the sum preformed by the GMAC does not act as a many-to-one mapping, i.e. that we can identify each centroid at the decoder and thereby split the interfering sources apart.

Without loss of generality, we choose encoder 2 to be *nested* in between encoder 1. We have

$$z = q_\Delta(x_1) + \alpha(\ell_{\pm c}[q_\Delta(x_2)]) + n, \quad (3)$$

where q_Δ represents a uniform mid-rise quantizer with stepsize Δ, $\ell_{\pm c}$ denotes the limitation to a certain (integer) value c and α is an attenuation factor. Further we let centroid no. i be denoted q_{i_m}

For a given Δ, c and α must be chosen small enough so that encoder 2 can be placed/nested in between encoder 1 (see Figure 2). This can be better understood by looking at the encoding process in more detail. We first quantize both sources

$$q_\Delta(x_m) = \left\lfloor \frac{x_m}{\Delta} \right\rceil = i_m(x_m), m = 1, 2 \quad (4)$$

where $\lfloor \cdot \rceil$ denotes rounding to the nearest integer. The second source is then limited to a certain $c \in \mathbb{N}$

$$\ell_{\pm c}[i_2(x_2)] = i_2(x_2) - c\left\lfloor \frac{i_2(x_2)}{c} \right\rceil = \check{i}_2(x_2). \quad (5)$$

Then $\check{i}_2$ is attenuated by a factor α in order to place the second encoder "in between" the first.

The basic concept is illustrated in Figure 2 (encoder 1 is included in the figure for clarity. Only the dots shows up in the real channel signal). When correlation is *low* (ρ_x close to 0), all centroids of encoder 2 lie between any two centroids

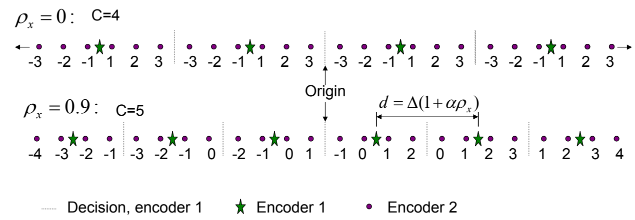

Figure 2: NQ structure in the channel space for $\rho_x = 0$ and 0.9.

of encoder 1. When the correlation is *high* ($\rho_x >\approx 0.7$), the centroids of encoder 2 will be *nested* in between the centroids of encoder 1. Note that not all centroids are re-used for every interval as is the case when $\rho_x \approx 0$. The correlation between the sources makes it possible to increase the resolution of both quantizers. Hence overall fidelity improves when ρ_x increases. At the decoder, we first compute an maximum likelihood (ML) estimate of the indices of the outer quantizer, followed by estimation of the inner quantizer index using the recovered first index. The ML estimate of the first source is

$$\begin{aligned} \tilde{x}_1 &= g_1(z) = q_{j_1(z)}, \qquad \text{where} \\ j_1(z) &= \arg\min_{j \in \mathbb{Z}} \|q_\Delta(j\Delta)(1 + \alpha\rho_x) - z\|^2, \end{aligned} \quad (6)$$

where the factor $(1 + \alpha\rho_x)$ takes into account that the midpoint for each *channel segment* (what lies between two decision borders for encoder one) shown in Figure 2 changes with ρ_x. That is, given that $q_{i_1(z)}$ is transmitted, the midpoint for the relevant channel segment is $q_{i_1(z)} + E\{\alpha x_2 | q_{i_1(z)}\} = q_{i_1(z)} + \alpha\rho_x q_{i_1(z)}$, where we used the relation $E\{x_2|x_1\} = \rho_x x_1$ for correlated Gaussian random variables [5, p. 233]. Given the first source, one can recover the second by:

$$\begin{aligned} \tilde{x}_2 &= g_2(z) = q_{\check{j}_2(z)}, \qquad \text{where} \\ \check{j}_2(z) &= \arg\min_{j \in \mathbb{Z}: |j| \leq \frac{c-2}{2}} \|z - q_{j_1(z)} - q_\Delta(j\Delta)\|^2. \end{aligned} \quad (7)$$

In order to minimize the MSE we calculate

$$\hat{x}_m = \mathbf{E}\{x_m | \tilde{x}_1, \tilde{x}_2\}, \qquad m = 1, 2 \quad (8)$$

The average transmit power from each encoder is

$$\begin{aligned} P_1 &= E[f_1(x_1)^2] = \sum_{i_1=-\infty}^{\infty} Pr(i_1) i_1^2 \\ P_2 &= E[f_2(x_2)^2] = \alpha^2 \sum_{\check{i}_2=-(c-1)/2}^{(c-1)/2} Pr(\check{i}_2)\check{i}_2^2 \end{aligned} \quad (9)$$

where $Pr(\cdot)$ is the probability for the event inside the parentheses. To design the optimal NQ, we need to determine the Δ, α and c that minimize D with respect to the given power constraints. Since the two encoders are asymmetric, P_1 is strictly greater than P_2, as one can see from (9). As stated in the introduction, we will optimize the codec in terms of received power constraint P_{Rx}. Time sharing can be applied to make the transmit power of each source averaged over long source symbols approximately equal.

Formally, we'll solve the following optimization problem

$$\min_{\Delta,\alpha,c:(P_1+P_2+2\rho_x\sqrt{P_1P_2})\leq P_{Rx}} D. \quad (10)$$

The average end-to-end distortion D can be broken into three independent distortion contributions: $D_{q,m}$, the quantization distortion, $D_{c,m}$, the distortion from limitation of source 2 and $D_{n,m}$, the distortion resulting from channel noise. The first two distortions can be seen as granular- and overload noise from the quantization process. Letting Nq_m denote the number of centroids for quantizer m (here $Nq_1 = \infty$ and $Nq_2 = 2(c-1)$) we get $\bar{\varepsilon}_q^2 = D_{q,m} + D_{c,m}$ and $\bar{\varepsilon}_q^2$:

$$\bar{\varepsilon}_q^2 = 2\sum_{i=1}^{\frac{Nq_m}{2}-1}\int_{(i-1)\Delta}^{i\Delta}\left(x_m-(i-1)\Delta-\frac{\Delta}{2}\right)^2 p_x(x_m)\mathrm{d}x_m + 2\int_{\left(\frac{Nq_m}{2}-1\right)\Delta}^{\infty}\left(x_m-\left(\frac{Nq_m}{2}-1\right)\Delta-\frac{\Delta}{2}\right)^2 p_x(x_m)\mathrm{d}x_m. \quad (11)$$

The last distortion term is

$$D_{n,m} = \iiint p_{\mathbf{x}}(x_1,x_2)p(z|i_1(x_1),\check{i}_2(x_2)) (\check{x}_m(i_1(x_1),\check{i}_2(x_2)) - \hat{x}_m(j_1(z),j_2(z)))^2\mathrm{d}r\mathrm{d}x_1\mathrm{d}x_2 = \sum_{i_1,\check{i}_2}\sum_{j_1,j_2} Pr(i_1,\check{i}_2)Pr(j_1,j_2|i_1,\check{i}_2)(\check{x}_m(i_1,\check{i}_2)-\hat{x}_m(j_1,j_2))^2, \quad (12)$$

where $\hat{x}_m$ is as previously defined and $\check{x}_m = E[\hat{x}_m|i_1,\check{i}_2]$ the quantized and limited source(s).

Better performance is possible if a different step-size is allowed for each quantizer, i.e. $\Delta_1 \neq \Delta_2$. One case we are particulary interested in is when $\Delta_2 \to 0$, that is, when encoder 2 becomes continuous. The resulting scheme is named *Scalar Quantizer Linear Coder* (SQLC) and is presented in following section.

2.2 Hybrid discrete-analog scheme: SQLC

Encoder 1 is the same as for NQ given in (4). Let centroid i be denoted q_i. For encoder 2, we now have $f_2 = \alpha(\ell_{\pm\kappa}[x_2])$, which is a limiter that clips the amplitude to $\pm\kappa$ where $\kappa \in \mathbb{R}_+$, followed by a scaling factor α. Like for the NQ, we must ensure that the sum of the quantized and the linear coded value is uniquely decodable. In order to do so, the second encoded source must be placed between the centroids of encoder 1 without overlapping with its "neighbors". The concept is depicted in Figure 3 for $\rho_x = 0$. Note that Figure 2 is a quantized version of the channel space structure shown in Figure 3.

The encoding function $f_1(x_1)$ is the same as for NQ, whereas $f_2(x_2) = \alpha(\ell_{\pm\kappa}[x_2])$. The decoders operate in a similar way as for the NQ. Source 1 is decoded as (6) then source 2 is found from

$$\tilde{x}_2 = g_2(z) = \beta(z - g_1(z)), \quad (13)$$

where β is an amplification factor. Again we compute $\hat{x}_m$ as in (8). The optimization problem is as in (10) except that we now optimize over α,β,Δ and κ.

We perform the distortion calculations in a somewhat different way than the NQ. Specifically, we must simplify (12)

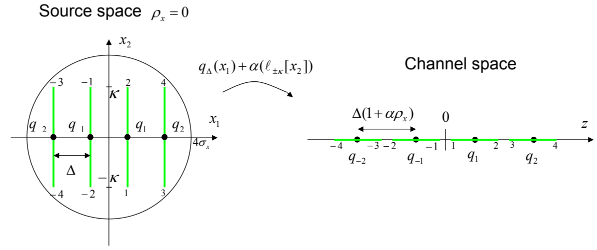

Figure 3: SQLC concept. The numbers show how the segments in the source- and channel space are related.

since the inner source is now continuous. We divide the average end-to-end distortion into the following five contributions (an approach inspired by Kotel'nikov [6, pp.62-98]): quantization distortion and channel distortion for source 1 and clipping distortion $\bar{\varepsilon}_{k2}^2$, channel distortion $\bar{\varepsilon}_{C2}^2$ and anomalous distortion $\bar{\varepsilon}_{an}^2$ for source 2.

The quantization distortion for source 1 is given by (11) with $Nq_1 = \infty$, the clipping distortion for source 2 is given by

$$\bar{\varepsilon}_{k2}^2 = 2\int_{\kappa}^{\infty}(x_2-\kappa)^2 p_x(x_2)\mathrm{d}x_2. \quad (14)$$

and the *channel distortion* for source 2 is

$$\bar{\varepsilon}_{C2}^2 = E\{(\tilde{x}_2-\hat{x}_2)^2\} = E\{(\tilde{x}_2-(\alpha\tilde{x}_2+n)\beta)^2\} \approx \sigma_x^2(1-\alpha\beta)^2+\beta^2\sigma_n^2 \quad (15)$$

where $\tilde{x}_2$ denotes the clipped source. The last approximation comes from assuming that $E\{\tilde{x}_2\} = \sigma_x^2$. In addition to channel distortion from the weak (additive/thermic) noise in (15), there is also the anomalous distortion resulting from a *threshold effect* [7], [8]. This is distortion on source 2 when the wrong centroid for encoder 1 is detected.

To calculate the anomalous distortion for source 2 and the effect of channel noise on source 1, we first need the channel output pdf. The pdf depends on ρ_x. As ρ_x increases, the limitation to $\pm\kappa$ becomes more and more insignificant since when ρ_x increases, the conditional pdf $p(x_2|x_1)$ narrows. That is, given a certain q_i, the correlation itself "limits" x_2 when ρ_x gets close to one. This can be seen by studying Figure 4 and Figure 3 together.

Assume first that ρ_x is small enough for the limitation to $\pm\kappa$ to be significant. Further let $y_2 = f_2(x_2)$, and $u(\cdot)$ be the Heaviside function. It is straight forward to show (using e.g. [5]) that the pdf of y_2 is

$$p_{y_2}(y_2) = \frac{1}{\sqrt{2\pi}\alpha\sigma_x}e^{-\frac{y_2^2}{2\alpha^2\sigma_x^2}}u(y_2-\alpha\kappa)u(-y_2+\alpha\kappa) + p_o\big(\delta(y_2-\alpha\kappa)+\delta(y_2+\alpha\kappa)\big), \quad (16)$$

where $p_o = Pr\{x_2 \geq \kappa\}$. When y_1 and y_2 are summed over GMAC, the resulting pdf (16) is centered at the transmitted centroid from encoder 1 (see Figure 3). Let z_2 denote the received signal when source 1 is subtracted. Assuming that the noise will not confuse the centroids of encoder 1, then the distribution after addition of noise is given by a convolution [5, 181-182].

$$p_{z_2}(z_2)_\kappa = p_{y_2} * p_n \quad (17)$$

The pdf for each channel segment is as in (17) until ρ_x becomes so large that the clipping to $\pm\kappa$ becomes negligible. Furthermore, y_2 will no longer be repeated on each segment, but spread out over several of the channel segments. This means that the channel segments shown in Figure 3 are no longer exact copies of each other but contains different "parts" of y_2 (see Figure 3 and Figure 4). This is the same effect as we saw for the NQ in Figure 2. We now have $y_2 \approx \alpha x_2$. Given

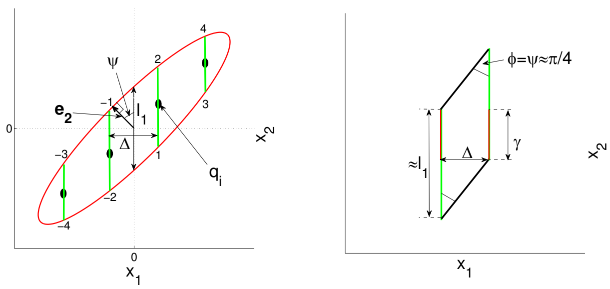

(a) (b)

Figure 4: SQLC when $\rho_x = 0.9$ 4(a) Structure in the source space. 4(b) How to calculate anomalous errors.

that q_i was transmitted one can show, using the expression for $p(x_2|x_1)$ [5, p.223], that $p_{z_2i}(z_2)_\gamma = p(y_2|q_i) * p_n(n)$ is

$$p_{z_2i}(z_2)_\gamma = \frac{e^{\frac{1}{2}\frac{(q_i(1+\alpha\rho_x)-z_2)^2}{(\alpha^2\sigma_x^2(\rho_x^2-1)-\sigma_n^2)}}}{\sqrt{2\pi(\alpha^2\sigma_x^2(1-\rho_x^2)+\sigma_n^2)}}. \quad (18)$$

The pdf in (17) is valid when $l_1 > 2\kappa$ while (18) is valid when $l_1 \le 2\kappa$. $l_1 = 2\|\mathbf{e}_2\|/\cos\psi = 2b\sqrt{\lambda_2}/\cos\psi$ as seen from Figure. 4(a). b (≈ 4) is a constant determining the width of the ellipse containing most of the probability mass and $\lambda_2 = \sigma_x^2(1-\rho_x)$ is the smallest eigenvalue of the covariance matrix C_x. The total channel output pdf can be found as a weighted sum of (18) or shifted and weighted versions of (17) depending on which of them is valid. The weighting is done with the probabilities for the centroids from encoder 1.

The anomalous distortion for source 2 can now be calculated. When the threshold effect happens, positive values are decoded as negative and vice versa, as seen from Figure 3. The magnitude of this error depends on whether $l_1 > 2\kappa$ or not. Consider first that $l_1 > 2\kappa$: The probability that anomalies happen is equal for each segment and given by

$$p_{th1} = 2\int_{\frac{\Delta}{2}(1+\alpha\rho_x)}^{\infty} p_{z_2}(z_2)_\kappa \mathrm{d}z_2, \quad (19)$$

where $p_{z_2}(z_2)_\kappa$ is given in (17). The error that occurs is bounded by $(2\kappa)^2$, since κ is detected as $-\kappa$ when anomalies first start to happen. Now consider that $l_1 \le 2\kappa$. It can be shown that the probability for anomalies is the same for each channel segment also for this case (given q_i) implying that

$$p_{th2} = 2\int_{\frac{\Delta}{2}(1+\alpha\rho_x)}^{\infty} p_{zi}(z_2)_{\gamma|q_i=0}\mathrm{d}z_2, \quad (20)$$

where $p_{zi}(z_2)_\gamma$ is given in (18). The error γ must be determined. γ can be bounded by considering jumps between the segments which are closest to the origin in the source (and channel) space since this results in the largest error. We can therefore use the parallelogram shown in Figure 4(b) as an approximation to determine γ when ρ_x is large. Since $\phi = \psi \approx \pi/4$ for large ρ_x, the parallelogram consists of a square and two triangles with both legs equal to Δ. We get

$$\gamma = l_1 - \Delta = 2b\sigma_x\sqrt{2(1-\rho_x)} - \Delta. \quad (21)$$

The anomalous distortion is therefore

$$\bar{\varepsilon}_{an}^2 \le \begin{cases} 4p_{th1}\kappa^2, & l_1 > 2\kappa, \\ p_{th2}\gamma^2, & l_1 \le 2\kappa. \end{cases} \quad (22)$$

Distortion from channel noise for source 1, $\bar{\varepsilon}_{C1}^2$, only occurs when the signal from source 2 and the channel noise together are larger than $\Delta/2$. Since we are only interested in finding the optimal parameters for designing the SQLC, we simplify the analysis by considering jumps to the nearest neighboring centroids only. The probability for this event is then the same as that in the case of the anomalous distortion for source 2 given by (19) and (20). Furthermore, the distortion we get when two neighboring centroids are interchanged is Δ^2, thus

$$\bar{\varepsilon}_{C1}^2 = \Delta^2 \begin{cases} p_{th1}, & l_1 > 2\kappa, \\ p_{th2}, & l_1 \le 2\kappa. \end{cases} \quad (23)$$

The average end-to-end distortion is then the sum of all the above distortion terms, divided by two. The power from encoder one is still as in (9) whereas the power from encoder 2 become

$$P_2 = \int_{-\alpha\kappa}^{\alpha\kappa} y_2^2 p_{y_2}(y_2)\mathrm{d}y_2 + 2p_o\alpha^2\kappa^2. \quad (24)$$

The optimization problem can now be solved. The resulting optimized parameters as a function of channel SNR must be found numerically but can be described by mathematical formulas using nonlinear curve fitting algorithms. What one can notice from the optimized parameters is that when ρ_x gets close to one we get a smaller Δ and a larger α for a given channel SNR compared to the $\rho_x = 0$ case. This implies improved fidelity (SDR) when ρ_x increases. Also, κ becomes irrelevant when ρ_x is close to one (since $p(x_2|x_1)$ narrows).

As discussed in Section 2.1, NQ can be roughly interpreted as a quantized version of the SQLC scheme, at least at high channel SNR. They both follow the same underlying principles, i.e. we can use similar geometrical arguments to explain the NQ as we did to explain the SQLC (picture a quantized version of Figure 3 and 4).

Although the SQLC has better performance than NQ in terms of SDR performance, as will be evident from Section 3, NQ is advantageous if we consider an extension of this scheme to more than two sources, or if a fully discrete system must be constructed.

3. SIMULATIONS

We compare the optimized NQ and SQLC to the performance (SDR) upper bound, the SSCC bound and the optimal distributed linear scheme (all derived in [1]). The channel SNR is defined as P/σ_n^2, where P is the average transmit power per

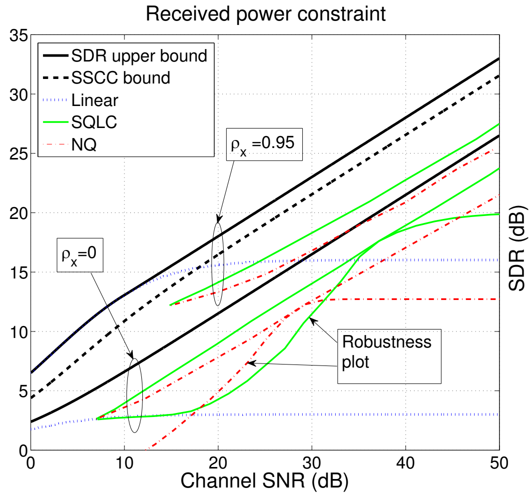

Figure 5: Comparison of relevant schemes

source symbol. Simulation results are shown in Figure 5 for $\rho_x = 0$ and $\rho_x = 0.95$. When $\rho_x = 0$ the SQLC is around 2-3 dB away from the performance upper bound and the NQ inferior to the SQLC by approximately 0-2 dB. Both schemes are significantly better than the linear scheme. Notice that the NQ and SQLC are robust to variations in noise variance.

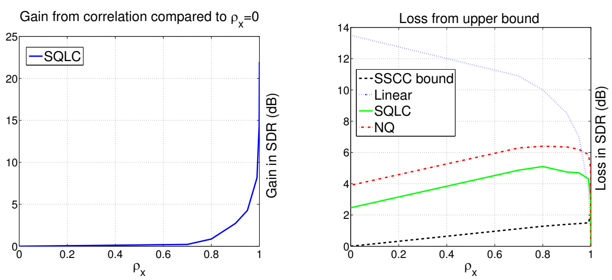

(a) (b)

Figure 6: How correlation affects performance.

It is also interesting that both the SQLC and NQ improve significantly with increasing ρ_x by only changing the parameters $\Delta, c, \kappa, \alpha$ and β, still using the same basic encoding and decoding principle. The gain from increasing ρ_x is shown in Figure 6(a) for the SQLC scheme at 30 dB channel SNR. Note also that there is no noticeable gain before $\rho_x \approx 0.7$, whereas the gain gets significant when $\rho_x \rightarrow 1$. The gap to the performance upper bound as a function of ρ_x is plotted in Figure 6(b) for 30dB channel SNR. When ρ_x gets larger, the performance of all schemes improve in terms of SDR. The gap to the performance upper bound in terms of SDR, however, becomes larger for the SQLC (≈5dB) and NQ (≈ 7dB). The opposite is true for the linear scheme. Considering that the mappings are delay free, the performance is still quite good. The SQLC, NQ and the linear scheme all reach the performance upper bound in the limit $\rho_x \rightarrow 1$, while the optimal SSCC scheme does not. The reason why the SQLC and NQ reach the performance upper bound is that when $\rho_x \rightarrow 1$, $\Delta \rightarrow 0$, and $\kappa, c \rightarrow \infty$. The result is then a linear scheme which is optimal when $\rho_x = 1$ [1].

Under an equal transmit power constraint one must expect a loss in performance for the SQLC and NQ since they have asymmetric encoders and are therefore optimal when $P_2 < P_1$. Simulations have shown that the loss from imposing equal transmit power constraint is around $0.5 - 1.5$ dB compared to the received power constraint case (with arbitrary P_i) when $\rho_x = 0$ and becomes less as ρ_x increases. The reason for this is that the two encoders become more "similar" as ρ_x increases. In the limit $\rho_x \rightarrow 1$ the two encoders become the same and no loss is observed relative to the received power constraint case.

4. SUMMARY

In this paper distributed delay free joint source-to-channel mappings for two memoryless Gaussian sources communicated over a Gaussian multiple access channel were proposed. The schemes were optimized for a received power constraint.

Both a fully discrete mapping based on nested quantization (NQ) and a hybrid discrete-analog scheme (SQLC) were analyzed. The SQLC has a performance 2 to 5 dB inferior to the performance upper bound, considering a received power constraint and the NQ is inferior to the SQLC with about 0 to 2dB. Both schemes are noise robust. Interestingly, both NQ and SQLC improve with increasing ρ_x without changing the basic encoder and decoder structure, and when $\rho_x \rightarrow 1$ both schemes reach the upper performance bound. Since the NQ and SQLC have nonsymmetric encoders, their performance will deteriorate somewhat when an equal transmit power constraint is imposed at each node.

Acknowledgment

This work was founded in part by the Research Council of Norway (NFR), under the projects MELODY nr. 187857/S10 and CROPS2 nr. 181530/S10 and the Swedish Research Council and VINNOVA.

REFERENCES

[1] A. Lapidoth and S. Tinguely, "Sending a bivariate Gaussian over a Gaussian MAC," *IEEE Trans. Information Theory*, vol. 56, no. 6, pp. 2714–2752, Jun. 2010.

[2] M. Gastpar, "Uncoded transmission is exactly optimal for a simple Gaussian "sensor" network," *IEEE Trans. Information Theory*, vol. 54, no. 11, pp. 5247–5251, Nov. 2008.

[3] S. D. Servetto, "Lattice quantization with side information: Codes, asymptotics, and applications in sensor networks," *IEEE Trans. Information Theory*, vol. 53, no. 2, pp. 714–731, Feb. 2007.

[4] M. Gastpar, "On capacity under receive and spatial spectrum-sharing constraints," *IEEE Trans. Information Theory*, vol. 53, no. 2, pp. 471–487, Feb. 2007.

[5] A. Papoulis and S. U. Pillai, *Probability, Random Variables and Stochastic Processes*, 4th ed. New York: McGraw-Hill higher education, Inc, 2002.

[6] V. A. Kotel'nikov, *The Theory of Optimum Noise Immunity*. New York: McGraw-Hill Book Company, Inc, 1959.

[7] C. E. Shannon, "Communication in the presence of noise," *Proc. IRE*, vol. 37, pp. 10–21, Jan. 1949.

[8] N. Merhav, "Threshold effects in parameter estimation as phase transitions in statistical mechanics." arXiv:1005.3620v1 [cs.IT], 2010.